

SD2AIL: ADVERSARIAL IMITATION LEARNING FROM SYNTHETIC DEMONSTRATIONS VIA DIFFUSION MODELS

Pengcheng Li¹ Qiang Fang^{1*} Tong Zhao¹ Yixing Lan¹ Xin Xu¹

¹ College of Intelligence Science and Technology, National University of Defense Technology, Changsha, Hunan, China

ABSTRACT

Adversarial Imitation Learning (AIL) is a dominant framework in imitation learning that infers rewards from expert demonstrations to guide policy optimization. Although providing more expert demonstrations typically leads to improved performance and greater stability, collecting such demonstrations can be challenging in certain scenarios. Inspired by the success of diffusion models in data generation, we propose SD2AIL, which utilizes synthetic demonstrations via diffusion models. We first employ a diffusion model in the discriminator to generate synthetic demonstrations as pseudo-expert data that augment the expert demonstrations. To selectively replay the most valuable demonstrations from the large pool of (pseudo-) expert demonstrations, we further introduce a prioritized expert demonstration replay strategy (PEDR). The experimental results on simulation tasks demonstrate the effectiveness and robustness of our method. In particular, in the Hopper task, our method achieves an average return of 3441, surpassing the state-of-the-art method by 89. Our code will be available at <https://github.com/positron-lpc/SD2AIL>.

Index Terms— Adversarial imitation learning, Diffusion model, Inverse reinforcement learning

1. INTRODUCTION

Imitation Learning (IL) learns policies directly from expert demonstrations without predefined reward signals [1, 2, 3], offering an alternative to Reinforcement Learning (RL), which often requires carefully designed reward functions that are difficult to obtain in certain scenarios.

Behavior Cloning (BC) [4, 5] employs supervised learning to simply and efficiently replicate expert actions. However, when encountering data outside the original expert distribution, BC tends to accumulate compounding errors. **Adversarial Imitation Learning (AIL)** [6, 7] can be regarded as a form of Inverse Reinforcement Learning (IRL) [2, 8], in which a reward function is first inferred from expert demonstrations, and the policy is then optimized by maximizing the inferred reward. GAIL [3] consists of a discriminator that distinguishes agent data from expert demonstrations and a generator that produces the policy. Moreover, researchers have introduced numerous improvements to AIL, such as refining the discriminator’s loss function [6], mitigating reward bias [7], and exploring alternative similarity metrics [9, 10].

Recently, diffusion models [11, 12], known for their powerful and flexible distribution modeling capabilities, have been introduced into RL. Diffuser [13] and BESO [14] leverage diffusion models to generate state-action trajectories. Diffusion-QL [15] integrates diffusion models into Q-learning to represent policies. DiffStitch [16]

employs diffusion models to synthesize trajectories for offline reinforcement learning. In addition, SMILING [17] proposes using a score function to approximate the expert distribution, thereby providing rewards for policy learning. Regarding AIL, DiffAIL [18] explores the use of diffusion models’ distribution modeling capabilities to enhance the discriminator in AIL, while DRAIL [19] employs a conditional diffusion model to replace the standard diffusion formulation. Although these approaches strengthen the discriminator in AIL, they primarily exploit the diffusion model’s loss and distribution modeling capabilities, overlooking its potential for data generation.

In AIL, providing more expert demonstrations typically leads to better performance and greater stability. However, compared to agent-environment interactions, expert demonstrations are often limited due to the high cost and difficulty of collection. Therefore, we propose fully utilizing the substantial amount of expert-like data generated by diffusion models.

In this paper, we propose a new approach Adversarial Imitation Learning from Synthetic Demonstration via Diffusion Models (SD2AIL). We retain a discriminator enhanced by a diffusion model but re-introduce the model’s powerful data generation capability. Specifically, we generate pseudo-expert demonstrations by selecting samples whose confidence scores exceed a specified threshold. These pseudo-expert demonstrations, combined with a small set of real expert demonstrations, are then utilized to train the discriminator in subsequent iterations. Inspired by Prioritized Experience Replay (PER) [20], we propose a novel Prioritized Expert Demonstration Replay (PEDR) mechanism to handle the large volume of (pseudo-) expert demonstrations in SD2AIL. By quantitatively measuring the importance of different (pseudo-) expert demonstrations, we prioritize more valuable demonstrations so that they are sampled more frequently. This strategy further enhances both the convergence speed and the learning efficiency of our model.

In summary, our contributions are as follows:

- We propose enhancing discriminator training through high-volume synthetic expert demonstrations generated by diffusion models.
- We introduce PEDR, a sampling strategy that replays critical (pseudo-) expert demonstrations more frequently during discriminator training.
- By combining the above two components, we propose SD2AIL and evaluate our method in four continuous control tasks using MuJoCo [21], achieving superior or competitive results compared to the baselines.

2. METHOD

In this section, we introduce our method SD2AIL, as shown in Fig. 1. First, we use high-quality samples generated by the diffusion model

*Corresponding Author

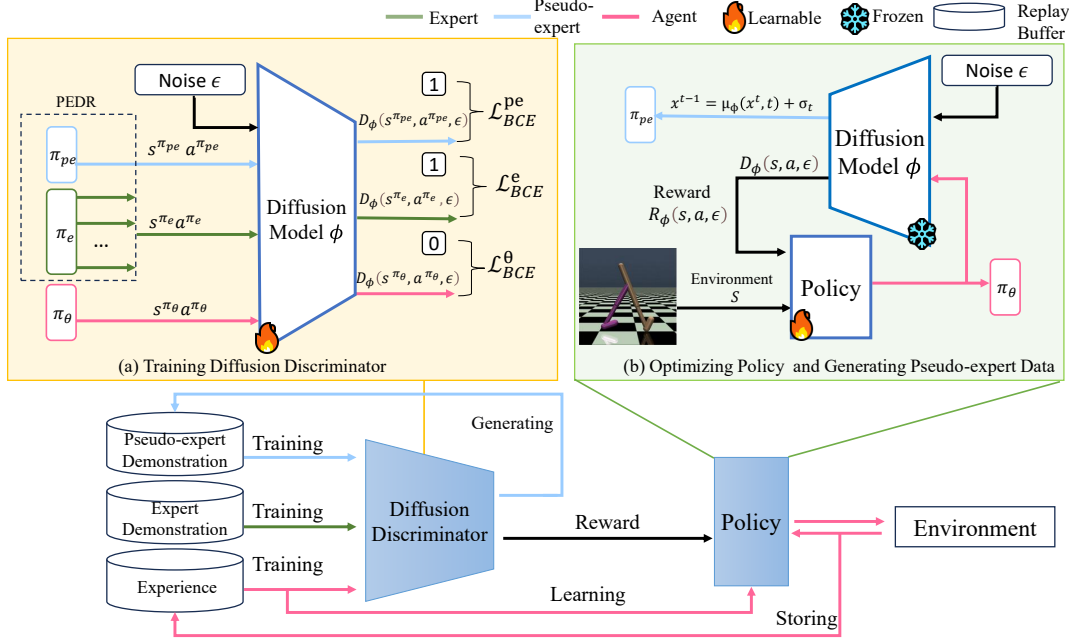


Fig. 1. SD2AIL. The overview of our proposed pipeline. (a) The diffusion discriminator D_ϕ samples expert demonstrations and pseudo-expert demonstrations using the prioritized expert demonstration replay method. The discriminator learns to differentiate between this data and the agent’s data. (b) During the optimization of the policy π_θ , the diffusion discriminator calculates the reward R from the output D_ϕ and generates pseudo-expert demonstrations during the denoising process. The policy network learns to maximize the reward from the discriminator. The generated pseudo-expert demonstrations are used for the next round of discriminator training.

as pseudo-expert demonstrations. The discriminator is then retrained with both expert and pseudo-expert demonstrations. Second, we introduce PEDR, which replays more valuable data more frequently from the large pool of (pseudo-) expert demonstrations.

2.1. Preliminaries in Diffusion-Based AIL

In diffusion-based AIL, the distribution modeling capability of diffusion models is leveraged to enhance the discriminator. Given a denoising step t and a state-action pair $(s, a) \in \mathcal{S} \times \mathcal{A}$, the diffusion model input is denoted as $x^t = (s_i, a_i)^t$, where \mathcal{S} and \mathcal{A} are the state and action spaces, respectively. Here, t denotes the diffusion step (superscript) and i the RL time step (subscript). The forward diffusion process injects noise into the data x^0 according to a variance schedule β^t . The reverse diffusion process learns to invert this corruption by predicting the added noise. The diffusion loss is defined as:

$$L(\phi) = \mathbb{E}_{t, x^0, \epsilon} \left[\left\| \epsilon - \epsilon_\phi \left(\sqrt{\bar{\alpha}^t} x^0 + \sqrt{1 - \bar{\alpha}^t} \epsilon, t \right) \right\|^2 \right] \quad (1)$$

where $\epsilon \sim \mathcal{N}(0, I)$, and ϵ_ϕ denotes the noise predicted by a neural network parameterized by ϕ . This diffusion loss is integrated into the discriminator. Therefore, the discriminator D_ϕ is defined as:

$$D_\phi(s_i, a_i, \epsilon) = \frac{1}{T} \sum_{t=1}^T \exp \left(-L_\phi(s_i^0, a_i^0, \epsilon, t) \right) \quad (2)$$

In fact, D_ϕ reflects the likelihood that (s, a) originates from expert demonstrations [17, 18, 19]. The corresponding surrogate reward is $R_\phi(s, a, \epsilon) = -\log(1 - D_\phi(s, a, \epsilon))$, which is used by reinforcement learning to optimize the policy.

2.2. AIL from Synthetic Demonstration via Diffusion Models

We re-utilize the generative capabilities of diffusion models. The diffusion model generates a large number of samples $x^0 = (s_i, a_i)^0$ by iteratively applying:

$$x^{t-1} = \mu_\phi(x^t, t) + \sigma_t \epsilon. \quad (3)$$

where $\mu_\phi(x^t, t) = \frac{1}{\sqrt{\alpha^t}}(x^t - \frac{\beta^t}{\sqrt{1-\alpha^t}}\epsilon_\phi(x^t, t))$ and $\epsilon \sim \mathcal{N}(0, I)$.

We consider the generated samples $(s_i, a_i)^0$ with a confidence $D_\phi(s_i, a_i)$ greater than a dynamic threshold τ as valid pseudo-expert demonstrations π_{pe} . The threshold is defined as:

$$\tau = \text{mean} [D_\phi(s_i^0, a_i^0, \epsilon)]. \quad (4)$$

In each iteration, we calculate the mean confidence from the expert demonstrations π_e to set a dynamic threshold τ . This allows us to use a lower threshold in the early stages of training to incorporate more pseudo-expert demonstrations, and increase the threshold in later stages to ensure the quality of the pseudo-expert samples. During each training of the discriminator, we sample demonstrations from π_{pe} and π_e in a specified ratio.

The optimization objective is then modified to:

$$\begin{aligned} \min_{\pi_\theta} \max_{D_\phi} & \mathbb{E}_{(s, a) \sim \pi_{pe}} [\log(D_\phi(s, a, \epsilon))] \\ & + \mathbb{E}_{(s, a) \sim \pi_e} [\log(D_\phi(s, a, \epsilon))] \\ & + \mathbb{E}_{(s, a) \sim \pi_\theta} [\log(1 - D_\phi(s, a, \epsilon))]. \end{aligned} \quad (5)$$

Here, $\mathbb{E}_{(s, a) \sim \pi_{pe}} [\log(D_\phi(s, a, \epsilon))]$ is an additional term representing the discriminator’s optimization objective for the pseudo-expert demonstrations. Here, we use the SAC algorithm for RL to optimize the policy, with the surrogate reward $R_\phi(s, a, \epsilon)$.

2.3. Prioritized Expert Demonstration Replay

The expert dataset, together with demonstrations generated by the diffusion model, provides a large pool of training data. Since these demonstrations vary in importance, we propose a prioritized expert demonstration replay (PEDR) mechanism for SD2AIL that increases the sampling frequency of more informative demonstrations to enhance convergence speed and learning efficiency.

We use the discriminator's error $\delta_i = 1 - D_\phi$ for the i -th (pseudo-) expert demonstration to measure its importance during training. The probability of sampling each expert data is given by:

$$P(i) = \frac{p_i^\zeta}{\sum_k p_k^\zeta}, \quad p_i = |\delta_i|. \quad (6)$$

Here, the parameter ζ controls the degree of prioritization. To reduce sampling bias, we apply importance sampling weights to adjust the discriminator's loss function, making the sampling process fairer. The importance sampling weight w_i is defined as:

$$w_i = \left(\frac{1}{N} \cdot \frac{1}{P(i)} \right)^\eta. \quad (7)$$

where the parameter η adjusts the importance sampling weights and is gradually annealed to 1 over time to stabilize the training process. Hence, the loss function of our discriminator is modified to the following form:

$$\begin{aligned} \mathcal{L}(\phi) = & w_i \mathcal{L}_{BCE}(-\log(D_\phi(s^{\pi_{pe}}, a^{\pi_{pe}}, \epsilon))) \\ & + w_i \mathcal{L}_{BCE}(-\log(D_\phi(s^{\pi_e}, a^{\pi_e}, \epsilon))) \\ & + \mathcal{L}_{BCE}(-\log(1 - D_\phi(s^{\pi_\theta}, a^{\pi_\theta}, \epsilon))) \end{aligned} \quad (8)$$

where \mathcal{L}_{BCE} denotes binary cross-entropy loss.

We establish N distinct prioritized replay buffers for the N expert trajectories and a single buffer for pseudo-expert demonstrations. This approach ensures that the discriminator's training is not biased toward any specific expert trajectory and guarantees the inclusion of both pseudo-expert and expert trajectories in every iteration.

The overall method is also summarized in Algorithm 1.

Algorithm 1 SD2AIL

Input: Expert demonstrations replay buffer \mathcal{R}_e , pseudo-expert demonstrations replay buffer \mathcal{R}_{pe} , policy network parameters θ , diffusion discriminator parameters ϕ , discriminator learning rate η_ϕ , batch size k , total time steps N .

- 1: **for** $n = 0, 1, 2, \dots, N$ **do**
- 2: Sample agent-environment interaction data (s, a, s') according to policy π_θ
- 3: Sample expert demonstrations $\{(s_i^{\pi_e}, a_i^{\pi_e})\}_{i=1}^k \sim \mathcal{R}_e$ and pseudo-expert demonstrations $\{(s_i^{\pi_{pe}}, a_i^{\pi_{pe}})\}_{i=1}^{7k} \sim \mathcal{R}_{pe}$ according to prioritized expert demonstration replay (6).
- 4: Calculate the output of the diffusion discriminator D_ϕ and compute the loss in (8).
- 5: Update the diffusion model: $\phi \leftarrow \phi - \eta_\phi \nabla \mathcal{L}$ via gradient descent.
- 6: Update the sampling probabilities for expert demonstrations (6).
- 7: Generate pseudo-expert samples (s, a) and add them to \mathcal{R}_{pe} .
- 8: Calculate the surrogate reward function $R_\phi(s, a, \epsilon)$.
- 9: Update the policy using SAC algorithm with the reward $R_\phi(s, a, \epsilon)$.
- 10: **end for**

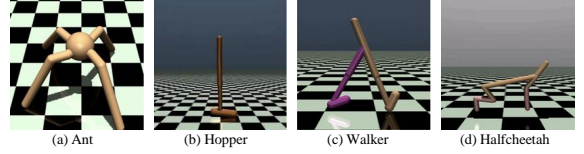


Fig. 2. Four classic continuous control tasks (Ant, Hopper, Walker and Halfcheetah) in MuJoCo

3. EXPERIMENTS

3.1. Experimental Setup

Dataset. As shown in Fig. 2, we evaluate the performance of our model on four classic MuJoCo tasks: Ant, Walker, Hopper, and HalfCheetah. All datasets consist of 40 trajectories, each containing 1,000 state-action pairs. Among these, the datasets for Ant, Walker, and HalfCheetah were provided by Kostrikov et al [26], while the Hopper dataset was provided by Wang et al. [18].

Details. Our experimental setup is based on DiffAIL [18]. Our diffusion model uses a total of $T = 10$ time steps with a linear scheduler. The ratio of sampling pseudo-expert demonstrations to expert demonstrations during each training session is 7:1. All experiments were run on a server equipped with three NVIDIA RTX A6000 GPUs.

3.2. Experimental Results

We compared our method with baseline methods on multiple classic MuJoCo tasks, including BC [1], GAIL [3], SMILING [17], DiffAIL [18], and DRAIL [19]. We randomly sampled 1, 4, and 16 expert trajectories from the dataset to serve as training demonstrations. Each experiment was repeated with five different random seeds, and we report the mean and standard deviation of the resulting performance. To improve readability, we applied a moving average with a window size of 5 to smooth the performance curves.

As shown in Fig. 3, under the 1-trajectory setting, our method achieved maximum environment rewards of 5345, 3441, and 5885 on the Ant, Hopper, and HalfCheetah tasks, respectively, exceeding those of human expert demonstrations, which were 4228, 3402, and 4663. In the Walker task, our method also achieved a result of 5743, surpassing the baselines. Notably, when there is only one expert trajectory, our method requires significantly fewer time steps to converge in the Hopper and HalfCheetah experiments, with about 210k and 180k steps, respectively. Our method outperforms DRAIL and SMILING across all four tasks, achieving higher final performance. While DRAIL employs a carefully designed single-step reverse diffusion process and achieves strong results on robot control tasks, this design may be better suited for large-scale training or settings with clear divergence between expert and policy behaviors. In more limited settings, especially when the distribution gap is small, the use of only one reverse diffusion step may limit its capacity to model expert behavior. Compared with AIL, which alternately trains the discriminator and the policy network, SMILING optimizes the score function and the policy separately during training. This decoupled optimization may prevent the two components from reaching their optimal performance simultaneously, thereby limiting its effectiveness in certain scenarios. Moreover, our method required significantly fewer training steps to converge and surpassed DiffAIL in three out of four tasks, achieving comparable results on Ant. This might be because each demonstration trajectory in the Ant expert

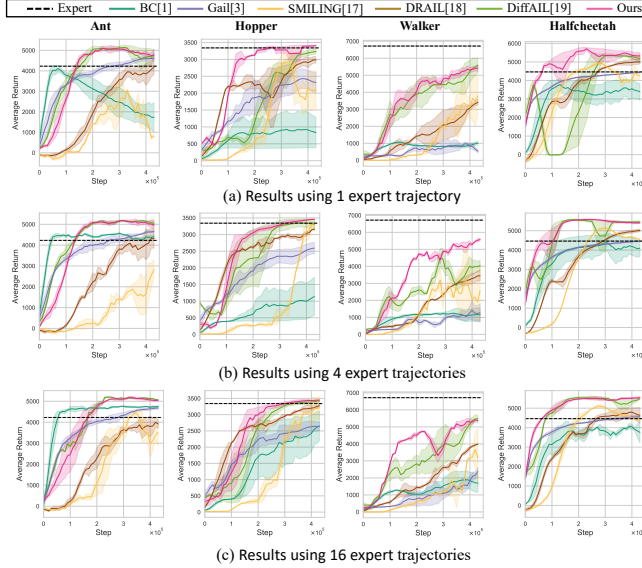


Fig. 3. Comparison of average returns on the Ant, Hopper, Walker, and HalfCheetah tasks, each run with five random seeds. Our method achieves faster convergence than the baselines in Hopper, Walker, and HalfCheetah.

dataset is of high quality and has sufficient diversity. Therefore, increasing the pseudo-expert demonstrations used for training did not lead to a significant improvement. Moreover, as the number of real expert trajectories increases, our method continues to improve its performance while requiring fewer training steps to converge.

3.3. Ablation Study

Visualization of Pseudo-Expert Demonstrations. To visualize and analyze the impact of the generated data, we randomly sampled a trajectory from the hopper expert demonstrations. We selected the action space for one joint of the hopper robot and applied Principal Component Analysis (PCA) to reduce the 11-dimensional state space to two dimensions. Subsequently, we generated 10,000 state-action pairs using the discriminator and visualized their distribution using the same methodology. Fig. 4 demonstrates that the generated pseudo-expert demonstrations exhibit a distribution similar to that of the genuine expert demonstrations. This additional synthetic data provides the discriminator with clearer training signals, which explains the effectiveness of our approach.

Quantitative Evaluation of Generated Sample Validity

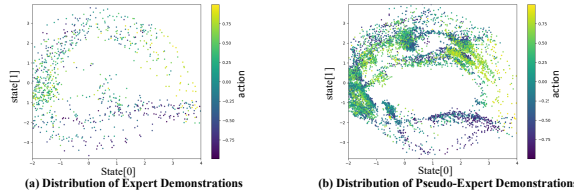


Fig. 4. Visualization of demonstrations. The pseudo-expert demonstrations exhibit a distribution similar to that of expert demonstrations. The additional data provides clearer guidance for the discriminator's training.

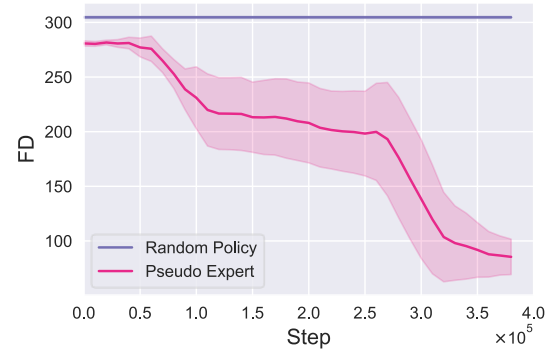


Fig. 5. FD to the expert demonstrations distribution for a random policy and pseudo-expert demonstrations. A smaller FD indicates greater similarity between the two distributions. The FD of the pseudo-expert demonstrations is significantly smaller than that of the random policy, indicating the validity of the generated samples.

Fréchet Distance (FD) is a commonly used evaluation metric in generative modeling [27]. It extracts image features using a pre-trained Inception network and measures the distribution discrepancy by computing the Fréchet distance in the feature space. A smaller FD indicates greater similarity between the two distributions. To obtain task-relevant features, we train a SAC agent in the Hopper environment and use the penultimate-layer features of its Q-network as the feature extractor. We then compute the FD between pseudo-expert and expert demonstrations in this feature space. For comparison, we also compute the FD between a random policy and the expert demonstrations using the same procedure. As shown in Fig. 5, the discrepancy between pseudo-expert and expert feature distributions gradually decreases as training progresses (reaching a minimum FD of 85.4), which is substantially lower than that of the random policy (FD = 304.7).

Correlation Between Surrogate Rewards and Real Rewards.

A more effective discriminator can provide a surrogate reward that is more closely aligned with the environment's reward. We analyzed the Pearson correlation coefficient (PCC) between the surrogate rewards and the environment's rewards. As shown in Fig. 6, the PCCs for our method are 93.0%, 90.1%, 92.3%, and 85.2% for the Ant, Hopper, Walker, and HalfCheetah tasks, respectively, while for DiffAIL, they are 92.2%, 77.4%, 81.3%, and 81.8%. This indicates that our surrogate reward function is more linearly correlated with the actual rewards, which facilitates more effective policy learning.

Effect of the Number of Denoising Timesteps. Generally, more denoising timesteps lead to higher quality generated samples.

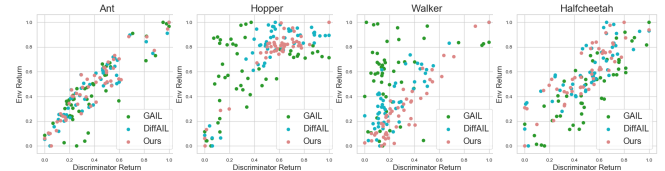


Fig. 6. Correlation between the discriminator return and the environment return. The return is normalized. Data points closer to the diagonal indicate a stronger positive correlation between the discriminator rewards and the environment rewards.

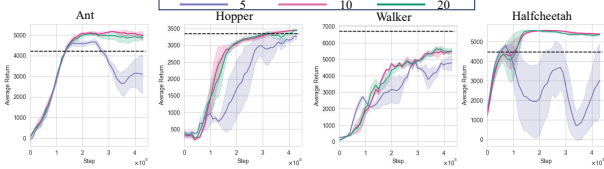


Fig. 7. The impact of different denoising timesteps on the results. Setting the denoising timesteps to 10 can balance the model results and the real time required for training.

In this experiment, we tested whether different numbers of denoising timesteps would affect the generated pseudo-expert demonstrations and thus the model performance. The experimental results in Fig. 7 show that increasing the number of denoising timesteps can effectively improve the final performance to a certain extent. When the number of denoising timesteps exceeds 10, further increasing this value only brings limited improvement and requires more time to complete the training.

Effect of Individual Components. We further conduct ablation studies to isolate the contributions of pseudo-expert demonstrations and PEDR in our method. For Pseudo-Expert Only, we evaluate the effect of pseudo-expert demonstrations alone and replace PEDR with random sampling. For PEDR Only, we use PEDR to replay expert demonstrations, while the generated pseudo-expert demonstrations are excluded from training. In the Walker environment, Fig. 8 shows that Pseudo-Expert Only achieves a peak average return of 4557 and PEDR Only achieves a peak average return of 4907, both outperforming DiffAIL. When both modules are combined, SD2AIL achieves the best overall performance.

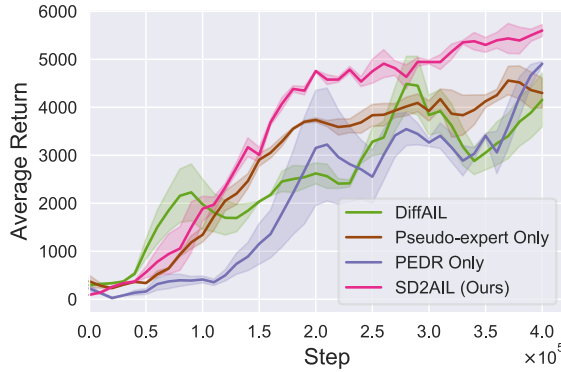


Fig. 8. Effect of Individual Components. Each component individually surpasses DiffAIL in average return, and when combined, SD2AIL achieves the best result.

4. CONCLUSIONS

In this work, we present SD2AIL, a novel Adversarial Imitation Learning from Synthetic Demonstrations via Diffusion Models. First, we adopt a diffusion model in the discriminator of AIL to generate pseudo-expert demonstrations that augment the real expert demonstrations. We further introduce a prioritized expert demonstration replay (PEDR) mechanism, selectively replaying the most valuable expert demonstrations from the large pool of (pseudo-)

expert data. We evaluate our method on several classic continuous control tasks, demonstrating competitive performance with fast and stable convergence. However, the use of diffusion models may relatively increase training time. In future work, we plan to further validate our method in real-world task scenarios.

5. REFERENCES

- [1] T. V. Samak, C. V. Samak, and S. Kandhasamy, “Robust behavioral cloning for autonomous vehicles using end-to-end imitation learning,” *SAE Int. J. Connected Autom. Veh.*, vol. 4, no. 3, pp. 279–295, 2021.
- [2] A. Y. Ng and S. Russell, “Algorithms for inverse reinforcement learning,” in *Proc. 17th Int. Conf. Mach. Learn.*, pp. 1–2, 2000.
- [3] J. Ho and S. Ermon, “Generative adversarial imitation learning,” in *Adv. Neural Inf. Process. Syst.*, vol. 29, 2016.
- [4] S. Ross, G. Gordon, and D. Bagnell, “A reduction of imitation learning and structured prediction to no-regret online learning,” in *Proc. 14th Int. Conf. Artif. Intell. Stat.*, pp. 627–635, 2011.
- [5] P. Florence, C. Lynch, A. Zeng, O. A. Ramirez, A. Wahid, L. Downs, A. Wong, J. Lee, I. Mordatch, and J. Tompson, “Implicit behavioral cloning,” in *Conference on Robot Learning*, Jan. 2022, pp. 158–168. PMLR.
- [6] J. Fu, K. Luo, and S. Levine, “Learning robust rewards with adversarial inverse reinforcement learning,” in *Proc. 6th Int. Conf. Learn. Represent.*, 2018.
- [7] I. Kostrikov, K. K. Agrawal, D. Dwibedi, S. Levine, and J. Tompson, “Discriminator-actor-critic: Addressing sample inefficiency and reward bias in adversarial imitation learning,” in *Proc. 7th Int. Conf. Learn. Represent.*, 2019.
- [8] L. Song, D. Li, and X. Xu, “Adaptive generative adversarial maximum entropy inverse reinforcement learning,” *Information Sciences*, vol. 695, p. 121712, 2025.
- [9] G. Freund, A. Gleave, and S. Levine, “A coupled flow approach to imitation learning,” in *Proc. 40th Int. Conf. Mach. Learn.*, pp. 10357–10372, 2023.
- [10] R. Dadashi, L. Hussenot, M. Geist, and O. Pietquin, “Primal Wasserstein Imitation Learning,” in *Proceedings of the International Conference on Learning Representations (ICLR)*, 2021.
- [11] J. Ho, A. Jain, and P. Abbeel, “Denoising diffusion probabilistic models,” in *Adv. Neural Inf. Process. Syst.*, vol. 33, pp. 6840–6851, 2020.
- [12] Y. Song, J. Sohl-Dickstein, D. P. Kingma, A. Kumar, S. Ermon, and B. Poole, “Score-based generative modeling through stochastic differential equations,” in *Proc. Int. Conf. Learn. Represent.*, 2021.
- [13] M. Janner, Y. Du, J. B. Tenenbaum, and S. Levine, “Planning with diffusion for flexible behavior synthesis,” in *Proc. 39th Int. Conf. Mach. Learn.*, 2022.
- [14] M. Reuss, M. Li, X. Jia, and R. Lioutikov, “Goal conditioned imitation learning using score-based diffusion policies,” in *Proc. Robot.: Sci. Syst.*, 2023.
- [15] Z. Wang, J. J. Hunt, and M. Zhou, “Diffusion policies as an expressive policy class for offline reinforcement learning,” in *Proc. Int. Conf. Learn. Represent.*, 2023.

- [16] L. Guanghe, Y. Shan, Z. Zhengbang, T. Long, and W. Zhang, “DiffStitch: Boosting offline reinforcement learning with diffusion-based trajectory stitching,” in Proc. 41st Int. Conf. Mach. Learn., 2024.
- [17] R. Wu, Y. Chen, G. Swamy, K. Brantley, and W. Sun, “Diffusing states and matching scores: A new framework for imitation learning,” in Proc. Int. Conf. Learn. Represent., 2025.
- [18] B. Wang, G. Wu, T. Pang, Y. Zhang, and Y. Yin, “DiffAIL: Diffusion adversarial imitation learning,” in Proc. AAAI Conf. Artif. Intell., vol. 38, no. 14, pp. 15447–15455, 2024.
- [19] C. M. Lai, H. C. Wang, P. C. Hsieh, F. Wang, M. H. Chen, and S. H. Sun, “Diffusion-reward adversarial imitation learning,” in Adv. Neural Inf. Process. Syst., vol. 37, pp. 95456–95487, 2024.
- [20] T. Schaul, J. Quan, I. Antonoglou, and D. Silver, “Prioritized experience replay,” in Proc. 4th Int. Conf. Learn. Represent., 2016.
- [21] E. Todorov, T. Erez, and Y. Tassa, “MuJoCo: A physics engine for model-based control,” in Proc. IEEE/RSJ Int. Conf. Intell. Robots Syst., pp. 5026–5033, 2012.
- [22] I. Goodfellow, J. Pouget-Abadie, M. Mirza, B. Xu, D. Warde-Farley, S. Ozair, A. Courville, and Y. Bengio, “Generative adversarial nets,” in Adv. Neural Inf. Process. Syst., vol. 27, 2014.
- [23] M. Andrychowicz, P. Wolski, R. Ray, J. Schneider, R. Fong, P. Welinder, et al., “Hindsight experience replay,” in Adv. Neural Inf. Process. Syst., pp. 5055–5065, 2017.
- [24] X. Cao, H. Y. Wan, Y. F. Lin, and S. Han, “High-value prioritized experience replay for off-policy reinforcement learning,” in Proc. IEEE 31st Int. Conf. Tools Artif. Intell., pp. 1510–1514, 2019.
- [25] T. M. Luu and C. D. Yoo, “Hindsight goal ranking on replay buffer for sparse reward environment,” IEEE Access, vol. 9, pp. 51996–52007, 2021.
- [26] I. Kostrikov, O. Nachum, and J. Tompson, “Imitation learning via off-policy distribution matching,” in Proc. 8th Int. Conf. Learn. Represent., 2020.
- [27] M. Heusel, H. Ramsauer, T. Unterthiner, B. Nessler, and S. Hochreiter, “GANs trained by a two time-scale update rule converge to a local Nash equilibrium,” in Adv. Neural Inf. Process. Syst., vol. 30, pp. 6626–6637, 2017.